Case Studies in Engineering Failure Analysis 5–6 (2016) 67–74

Contents lists available at ScienceDirect

Case Studies in Engineering Failure Analysis

journal homepage: www.elsevier.com/locate/csefa

Case study

Failure analysis of mixed mode crack growth in heavy duty truck frame rail

Vinay N. Rao *, Jeffrey W. Eischen

North Carolina State University, Raleigh, 27606 NC, USA

ARTICLE INFO

Article history:
Received 18 January 2016
Received in revised form 12 March 2016
Accepted 29 March 2016
Available online 6 April 2016

Keywords:
Fatigue
Frame rail failure
Crack growth simulation
Fracture
Finite element analysis

ABSTRACT

A failure analysis investigation was performed on a fractured heavy duty truck frame rail obtained during endurance track testing. The fracture observed was on the frame web within the torque rod connection to the rear drive axle of the vehicle. This section of frame experiences multi-axial loading conditions including out-of-plane bending, twisting and shear under road loads. Metallographic examination revealed micro-cracks on the edges of an open hole located in an area of high stress concentration. This manufacturing defect acted as a stress raiser and resulted in fatigue crack initiation. Simulation of crack growth on frame rail using dynamic loads from a full vehicle model was completed. After careful analysis it was concluded that the failure occurred due to an aggressively drilled open hole which created small crack initiations in a high stress-state location of the frame. This resulted in extensive curvilinear crack growth under dynamic loads of the vehicle.

1. Introduction

A failure in a heavy duty truck frame generally involves crack growth under mixed mode I/II/III loading since the vehicle loads are highly nonlinear transient and multi-axial with large deformation behavior. This is similar to many mixed mode crack growth problems reported in literature [1–9]. The propagation of cracks in truck frame members is important to be well studied since on reaching critical crack lengths it can lead to complete breakdown of the vehicle and this may lead to catastrophic accidents with loss of life. Although there are routine vehicle inspections currently in place to detect and repair/replace fatigue cracked components, the ability to better predict crack path and orientation under various loading conditions can help avoid expensive losses and improve the design with better durability.

In this work, failure analysis of frame rail crack was carried out. Through careful macroscopic and microscopic observations, the crack was found to be primarily caused due to aggressively drilled open-hole close to an existing bolt hole. The drilled hole created small crack initiations within a high stress location of the frame. FRANC3D crack growth simulation tool combined with NASTRAN finite element solver was used in this work to simulate frame crack growth under full vehicle dynamic loads. The simulation results obtained showed good correlation to physical crack path and cycles to failure.

---

* Corresponding author. Tel.: +1 2604456357.
E-mail address: vnrao@ncsu.edu (V.N. Rao).

http://dx.doi.org/10.1016/j.csefa.2016.03.002

2. Experimental procedure

Depending on the operational class to which the vehicle is used different testing events are selected. Fig. 1 provides schematic representation for some of the endurance test events used for full vehicle validation.

Endurance testing is done at different speeds and at different gross vehicle weight rating (GVWR). These test events provide dynamic interactions between different vehicle modules and sub-systems, enables dynamic interference and clearance check. The test vehicle will be instrumented with strain gages, load transducers and accelerometers to measure vehicle response during testing. The data measured (strain, displacement and acceleration history) are used to validate new designs and improve numerical model development. The damage obtained during test will be scaled for repeated cycles to estimate cycles to failure. The accelerated damages and wear obtained on different vehicle parts are then inspected and studied to follow up with design modifications.

3. Experimental results

3.1. Visual inspection

During a full vehicle endurance test repeated inspections were carried out after every few cycles of testing, after certain test cycles frame fatigue cracks were noticed during inspection near the rear drive axle torque rod connection of the vehicle. Fig. 2(a) shows the layout of the vehicle and the area of failure noticed on the vehicle. In Fig. 2(b), the torque rod bracket attachment to the inner web of frame with a reinforcement plate is shown. There were visible cracks on the frame extending behind the reinforcement plate and on either side of the torque rod bracket. In Fig. 2(c), the reinforcement plate bolted on both inner and outer section of frame was removed to view the crack path. This shows a bolt–hole being drilled near an existing bolt and cracks originating from this location.

Fig. 3(a) reveals the complete range of failure with the crack path taking a curvilinear route behind the reinforcement plate and multiple cracks originated at the open drilled hole. It was observed there were two open holes present close to bolted holes and the presence of open holes were not realized during testing with the reinforcement plate installed. The open hole in the middle did not seem to affect the crack growth and was observed to be present in a low stress area. A closer view of exposed crack surfaces shows primary and secondary failure origins in Fig. 3(b). In Fig. 3(b), beach marks were identified and this indicated a fatigue failure mechanism.

3.2. SEM observation

Fig. 4 shows primary crack initiations originated at the edge of the bolt hole and the secondary crack initiations originated on the inner surface of the frame adjacent to the bolt hole. In Fig. 5(a), a low magnification SEM image shows the beach marks (above the red dashed lines) indicative of a fatigue crack growth mechanism. Fig. 5(b) shows higher magnification optical micrograph image of the cracks on the bolt–hole wall which resulted from the aggressive hole drilling process.

A chemical analysis was performed on the frame section using an Optical Emission Spectrometer (OES). The chemical composition of frame section was found to be consistent with the test requirement. The base metal hardness of the frame section was found to be 32 HRC in rockwell hardness, which was in the reasonable hardness range for quenched and tempered low carbon/manganese/boron steel.

Rough road profile High gradient topography

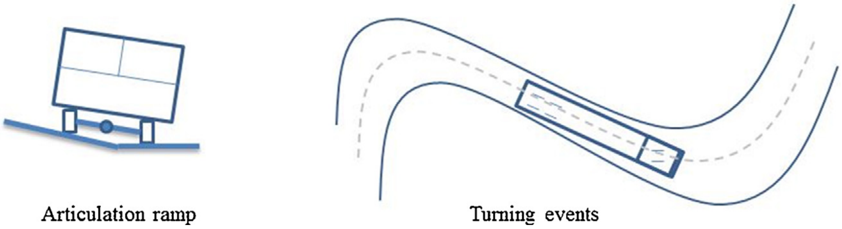

Articulation ramp Turning events

Fig. 1. Full vehicle endurance test events.

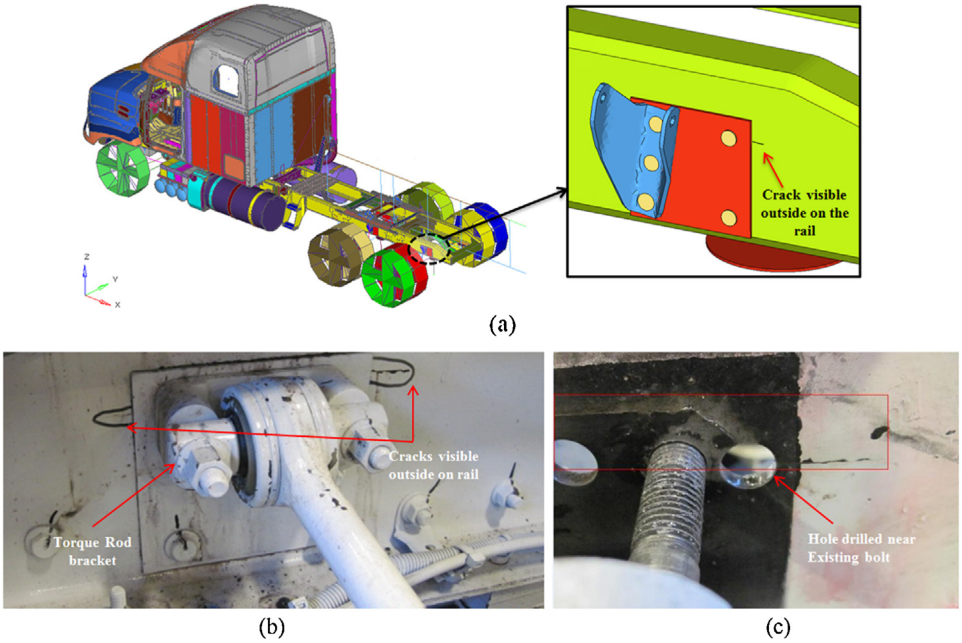

Fig. 2. (a) Full vehicle layout and failure location. (b) Frame cracks visible near torque rod connection. (c) Crack path visible on frame behind outer reinforcement plate.

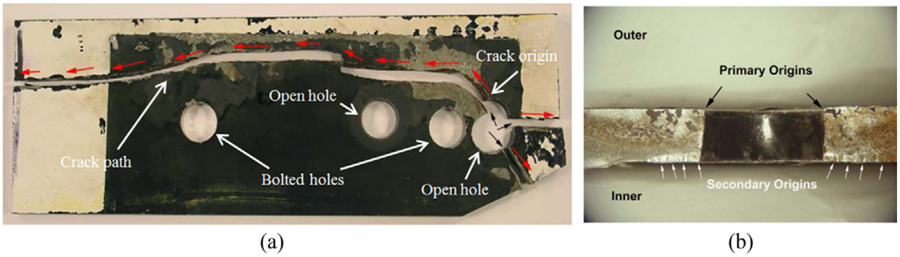

Fig. 3. (a) Complete crack propagation directions on frame section. (b) Failure origin on analysis.

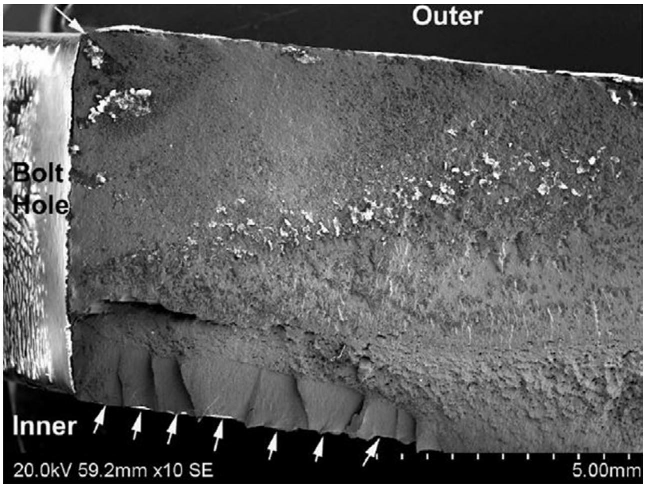

Fig. 4. Crack origins on inner and outer surface.

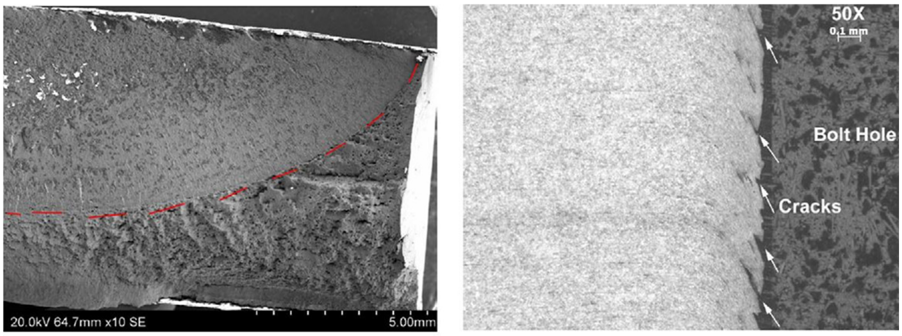

(a) (b)

Fig. 5. (a) SEM image showing beach marks. (b) Optical micrograph showing cracks on the wall of open hole.

4. Simulation results

Fig. 6(a) shows the interface forces applied on the sub-model used for fatigue and crack growth simulation. The interface forces were applied on all the grid points defining the boundary of the sub-model with the full vehicle model. The loads were obtained from modal transient analysis of a full vehicle model for multi-axial test track excitations. Fig. 6(b) shows displacement plot indicating frame twist and bend modes obtained under multi-axial loading.

Fig. 7(a) shows von-Mises stress plot on the frame using full vehicle response dynamic loads. The stress obtained exceeded material yield strength at the open-hole and near the crack path obtained in physical test. A fatigue analysis for the duty cycle of test track events provided a damage value of "1.1" with the acceptance criteria being "0.5". Fig. 7(b) shows FRANC3D meshed model with a small semi-elliptical crack (0.5 mm) inserted at the edge of open-hole and located in an area of high stress concentration. The size of the initial crack inserted was chosen assuming the surface cracks inserted during aggressive drilling process will grow to that size in few loading cycles and crack growth from there onwards was of primary interest.

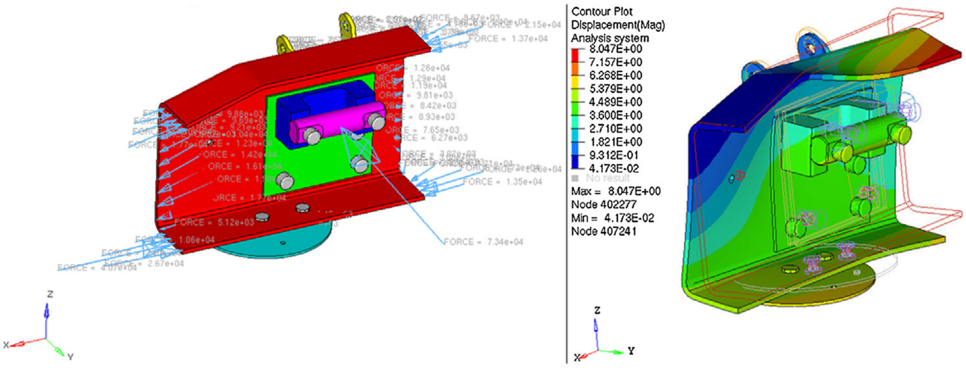

(a) (b)

Fig. 6. (a) Multi-axial loading on frame section. (b) Displacement plot under multi-axial loads.

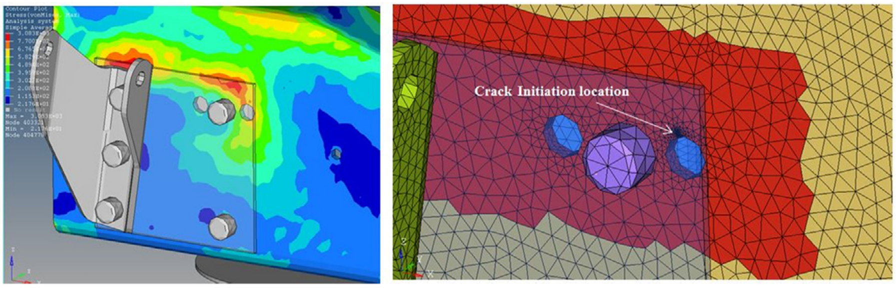

(a) (b)

Fig. 7. (a) Von-Mises stress plot obtained on frame. (b) FRANC3D model with initial crack location.

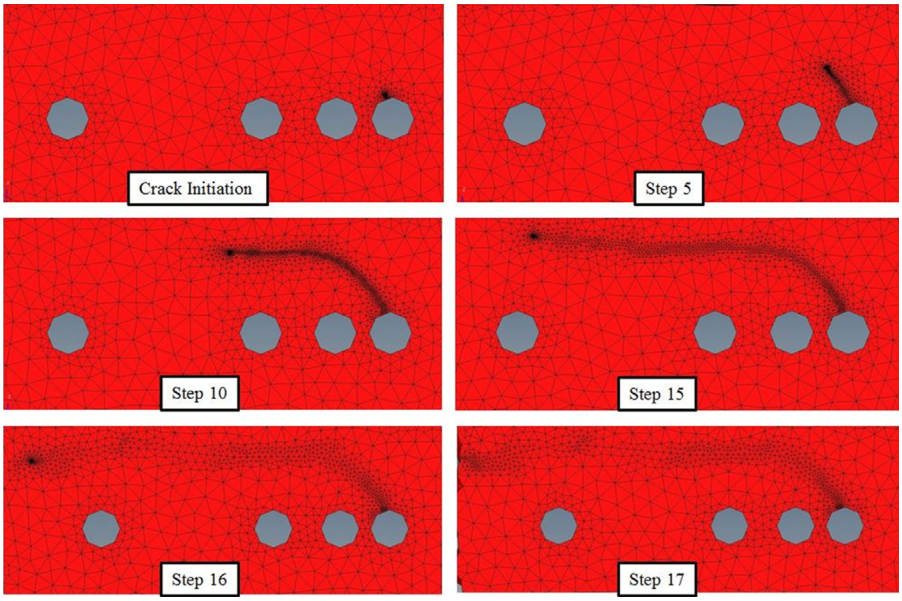

Fig. 8. Crack growth steps showing crack extension on frame.

In Fig. 8, crack growth history is shown where each step requires computing stress intensity factors (SIF) after growing the crack in FRANC3D and using NASTRAN solver for finite element analysis. The loads used for crack growth simulation were from full vehicle response dynamic loads and the 3D crack growth was chosen to be for constant amplitude fatigue type. The crack kink angle was determined using the strain energy release rate method. The well-known “Paris law” was used for fatigue growth rate model and the coefficients for Paris law were obtained from the frame supplier [10] (coefficient $C = 6 \times 10^{-8}$, exponent $m = 2.26$, $K_{\text{threshold}} = 316.2\ \text{MPa}\sqrt{\text{mm}}$). Stress intensity factors (SIF) were computed using the “Interaction Integral” (M-Integral) method and include effects of crack face contact and crack pressure.

5. Discussion

Based on the visual inspection and metallographic examination it was confirmed that the curvilinear crack growth on the frame rail was a fatigue failure and crack initiations was due to a poor quality drilled hole on the frame. The crack path obtained was influenced by mixed-mode stress intensity factors. The simulation results obtained were used to understand the root cause of failure and can be used to recommend design modifications to prevent such extensive fatigue failure of heavy duty truck frame.

The damaging loads identified were primarily from vehicle turning events which results in rear drive axle torque rod pushing the torque rod bracket into the web of frame section, causing an out-of-plane bending as shown in Fig. 9(a). This out of plane bending loads causes any cracks present on the outer frame surface to open and grow under Mode I type crack growth behavior. Fig. 9(b) shows crack opening (scaled 10 times) at step 17 under out-of-plane bending loads on frame.

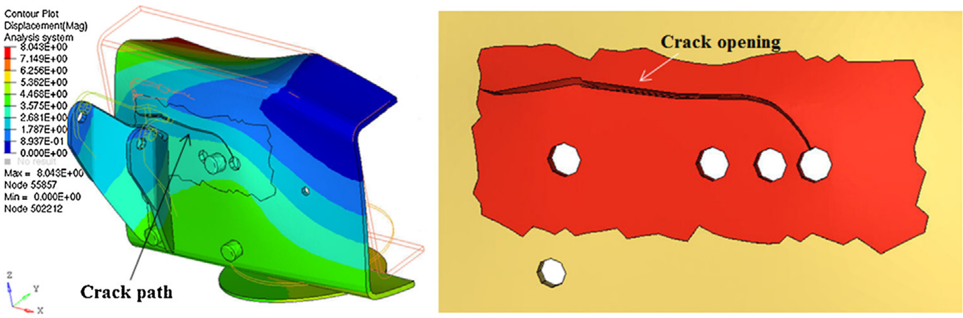

(a) (b)

Fig. 9. (a) Out-of-plane bending of frame during turning event. (b) Crack opening under frame bending loads.

Fig. 10 shows comparison of crack path obtained between physical test and full vehicle response based 3D crack growth simulation result. It can be seen that the curvilinear mixed-mode crack path simulated has good agreement with physical test result. The primary crack path was observed to follow high stress zone as identified in simulation result, the secondary crack paths were not considered during simulation.

5.1. Sensitivity analysis of frame open-hole location

The objective of this sensitivity study was to determine the effect of moving the open-hole on frame that had been drilled close to an existing bolt (high stress area) further from its initial location in order to determine if maintaining a certain distance from the high stress area will be identified to prevent fatigue failure. In Fig. 11, description of design iterations performed for sensitivity study is shown. The frame open-hole was moved along "*X*" direction in multiple increments and the distribution of stress concentration near open-hole was studied. It is to be noted that frame holes are often drilled to mount brackets and for routing of hydraulics and electrical wires. This study helps identify no-drill zone based on both safe life and fracture mechanics perspective.

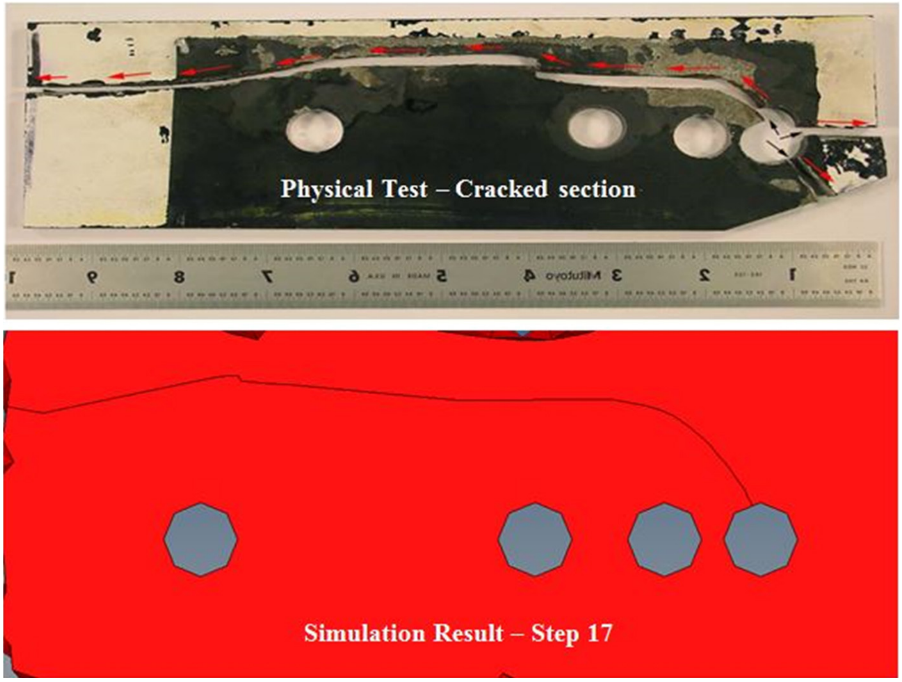
Physical Test – Cracked section

Simulation Result – Step 17

Fig. 10. Frame crack during physical test compared with simulation result obtained using full vehicle response based 3D crack growth process.

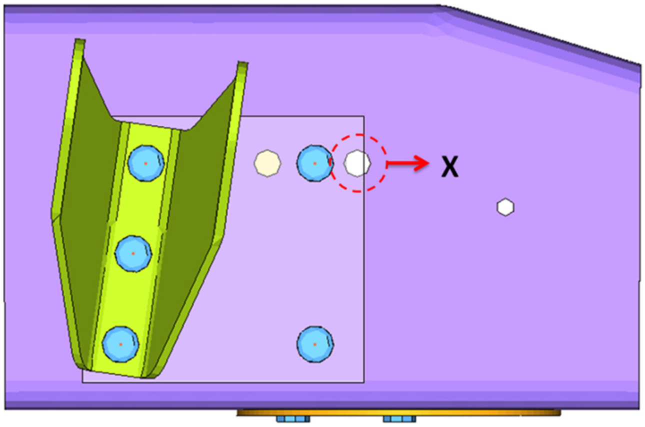

Fig. 11. Location of frame open-hole moved along "*X*" direction for sensitivity study.

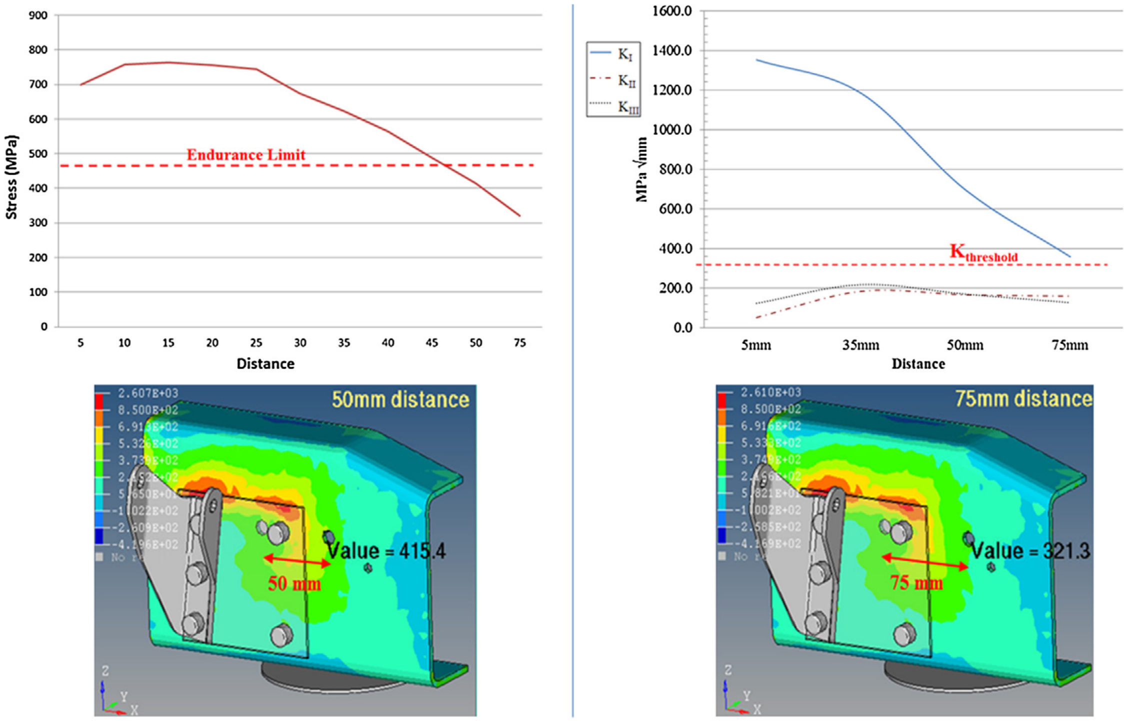

(a) (b)

Fig. 12. (a) Safe life approach and (b) damage tolerant approach results for sensitivity study.

The endurance strength (1E6 cycles) of the frame was found to be 2403 μ (microns) [10] corresponding to a stress of 478 MPa. From the stress based design the allowable open-hole location was found to be around 45 mm from its initial location, as shown in Fig. 12(a). However the fracture mechanics approach was necessary to ensure a reliable location for frame holes.

The fracture mechanics approach involves inserting small semi-elliptical surface crack at different open-hole locations and extracting maximum stress intensity factors along crack fronts. It was observed K_I drops linearly with distance and approaches $K_{\text{threshold}}$ at a distance of around 75 mm from its initial location. In Fig. 12(b), K_I remains above $K_{\text{threshold}}$ at 45 mm and an aggressive open-hole would still lead to crack propagation under fatigue loading at that distance. This study provides a comparative view of two design approaches and helps identify a no drill zone on frame rails near high stress areas.

6. Conclusions

Based on the experimental observations and simulation results, it can be concluded that an aggressively drilled open hole created small crack initiations in a high stress-state location of the frame, which resulted in extensive curvilinear crack growth under dynamic loads of the vehicle. The FRANC3D crack propagation tool combined with NASTRAN finite element solver predicted crack path similar to physical test failure and provided a good correlation for cycles to failure. A sensitivity study was done to identify safe zone for open holes and would help specify restrictions on frame hole drilling. The present work provides successful methodology applied to failure analysis of frame rail cracks in heavy duty trucks, which may also be applied for other engineering failure analysis problems.

Acknowledgements

The research presented here was partially carried out at the Advanced Calculations group of Chassis Vehicle Dynamics and Engineering (CVDE) section of Volvo Group North America, Greensboro, North Carolina, USA. The authors would like to thank Dr. Omar Ibrahim at Process Optimization Corporation for providing support and license for FRANC3D program in this research.

References

[1] Sih GC. Strain-energy-density factor applied to mixed mode crack problems. Int J Fract 1974;10(September (3)).

[2] Chao Y-J, Zhu X-K. A simple theory for describing the transition between tensile and shear mechanisms in mode I, II, III and mixed-mode fracture. Mixed-mode Crack Behav ASTM STP 1999;1359:41–57.

[3] Yates JR, Zanganeh M, Tomlinson RA, Brown MW, Diaz Garrido FA. Crack paths under mixed mode loading. Eng Fract Mech 2008;75:319–30.
[4] Davis BR, Wawrzynek PA, Ingraffea AR. Simulation of arbitrary mixed-mode crack growth using an energy-based approach.In: Conference proceedings of the society for experimental mechanics series. Fract Fatigue Fail Damage Evol 2015;5:1–9.
[5] Seifi R, Eshraghi M. Effects of mixed-mode overloading on the mixed-mode I+II fatigue crack growth. Arch Appl Mech 2013;83(July (7)):987–1000.
[6] Seifi R, Omidvar N. Fatigue crack growth under mixed mode I+III loading. Mar Struct 2013;34:1–15.
[7] Miller EE, Sutton MA, Deng X, Watts H, Reynolds AP, Ke X, et al. Experimental and predicted crack paths for Al-2024-T351 under mixed-mode I/II fatigue.In: Conference proceedings of the society for experimental mechanics series. Fract Fatigue Fail Damage Evol 2015;5:11–20.
[8] Deng X, Ke X, Sutton MA, Watts HS, Schreier HW. Curvilinear fatigue crack growth under out-of-phase loading conditions.In: Conference proceedings of the society for experimental mechanics series. Fract Fatigue Fail Damage Evol 2015;5:27–34.
[9] Fremy F, Pommier S, Poncelet M, Raka B, Galenne E, Courtin S, et al. Load path effect on fatigue crack propagation in I+II+III mixed mode conditions – Part 1: Experimental investigations. Int J Fatigue 2014;62:104–12.
[10] Fleming S. Fatigue crack growth for typical CV siderail hole-making processes applied to heat-treated steel (MET1123) and ultra-high strength low alloy steel (120XF). SAE International; 2009, 2009-01-2863.